

Assessment of Coating Performance on Waterwalls and Superheaters in a Pulverised Fuel-Fired Power Station

Nigel Simms¹ · Maud Seraffon² · Andy Pidcock¹ · Colin Davis²

Received: 20 November 2016

© The Author(s) 2017. This article is published with open access at Springerlink.com

Abstract Protective coatings offer one route to increase the lives of heat exchangers in pulverised fuel power plants. A range of candidate coatings have been exposed on the waterwall and superheaters of a 500 MWe UK power station unit for periods of up to ~ 4 years (24,880 operating hours), during which time this unit was fired on a mixture of UK and world-traded coals. Both nickel- and iron-based candidate coatings were included, applied using high velocity oxy-fuel or arc-wire process; a selection of these also had a surface sealant applied to investigate its effectiveness. Dimensional metrology was used to evaluate coating performances, with SEM/EDX examinations used to investigate the various degradation mechanisms found. Both the waterwall and superheater environments generated their characteristic corrosion damage morphologies which depended on the radial positions around the tube. Coating performances were found to depend on the initial coating quality rather than composition, and were not improved by the use of a sealant.

Keywords Coatings · Fireside corrosion · Pulverised fuel combustion · Waterwalls and superheaters

✉ Nigel Simms
n.j.simms@cranfield.ac.uk

Maud Seraffon
maud.seraffon@uniper.energy

Andy Pidcock
andy.pidcock@cranfield.ac.uk

Colin Davis
colin.davis@uniper.energy

¹ Cranfield University, Cranfield, Bedfordshire MK43 0AL, UK

² Uniper Technologies Ltd, Ratcliffe-on-Soar, Nottingham, Nottinghamshire NG11 0EE, UK

Introduction

Pulverised coal-fired power stations currently produce much of the electricity used in the world, but they also generate CO₂ emissions and often have efficiencies of only ~35 to 40% [1]. To increase the efficiencies of this technology and reduce its CO₂ emissions, it is necessary to increase the fluid temperatures and pressures within its steam circuit. Most existing power systems use superheated steam at 560–580 °C/160–180 bar, with new state of the art systems using 610–620 °C/250–300 bar; future systems are being considered with steam temperatures of 650, 700 or 760 °C (and pressures of up to ~350 bar) [2–5]. CO₂ emissions can be reduced independently by introducing biomass-co-firing, but this requires the increased fuel costs to be balanced by subsidies (and/or regulations). However, fuel costs can sometimes be reduced by using world-traded coals instead of those mined locally. In the future, post-combustion CO₂ capture systems offer the potential to further reduce emissions, but these need to be coupled with increased steam conditions to maintain the overall system efficiencies. From a materials point of view, potential changes to heat exchanger operating environments from the use of different fuels and increased steamside temperatures need careful consideration as they may increase component degradation rates causing higher maintenance costs and increasing the chance of component failures (causing expensive unplanned outages) [3–7]. The use of alternative materials (coatings and base alloys) needs to be considered and investigated in both laboratory and available plant environments.

As new specifically tailored coatings can take 5–10 years to develop and represent a significant investment, candidate coatings for more rapid introduction into pulverised coal (mostly)-fired power systems need to be those that can be manufactured from commercially available products (e.g. powders/wires) and use established coating techniques. Coatings have traditionally been used in much smaller waste or biomass-fired power stations (based on grate or fluidized bed technologies), with alloys such as 625 or 622 (applied using weld overlay or laser processing) being used to resist chloride-dominated fireside corrosion at the lower metal temperatures associated with these lower efficiency systems. However, coal-fired systems have traditionally preferred the use of higher alloyed steel tubes to replace corroded areas (although there are examples of co-extruded tubes and air-plasma sprayed Ni-50Cr coatings being used in UK power stations). A particular challenge in using coatings to protect heat exchanger surfaces within pulverised coal-dominated power plants is maintaining the coating quality over the large heat exchanger areas. In addition, coatings that may be successful in resisting sulphate-dominated fireside corrosion on coal-fired superheaters at 600–650 °C may not be successful in resisting other forms of high-temperature corrosion (e.g. on waterwalls); this is a result of the different exposure conditions, metal surface temperatures and resulting corrosion mechanisms that are found on the various types of heat exchangers [7].

This paper reports the results of the long-term exposure of a selection of candidate protective coatings on the waterwalls and superheater tubes within a 500 MWe pulverised fuel-fired unit of a UK power station. These coatings were

manufactured and installed during a plant outage in 2011, as part of the UK ASPIRE R&D project. The coatings were then exposed for 24,880 operating hours before being removed and examined during the unit's next major outage in 2015, as part of the EU NEXTGENPOWER R&D project. During this exposure, the power plant was fired using a mixture of UK and world-traded coals. The selection of coatings deliberately contained a range of compositions, but was mostly applied using high-velocity oxy-fuel (HVOF), with one coating composition being applied using arc-wire. In addition, the effectiveness of using a candidate surface sealant was investigated on each of the different coating compositions. Following their exposures, the tubes were subjected to visual and destructive examinations. Dimensional metrology was used to evaluate coating performances, with SEM/EDX examinations used to investigate the various degradation mechanisms found.

Such data can be used in conjunction with the results of the SEM/EDX examinations of the degradation mechanism to determine the best candidate coating systems. It was found that initial (i.e. as-received) coating quality was particularly important in determining the performance of the coatings. In addition, there were significant differences between the performances of coatings in the waterwall and superheater environments.

Experimental Procedures

Power Plant Tube Sample Locations

Tubes were installed into one waterwall and two superheaters of a 500 MWe unit of a UK pulverised coal-fired power station (Fig. 1). For the waterwall, an ~ 3 m long furnace wall panel, consisting of ten carbon steel tubes with outer diameter

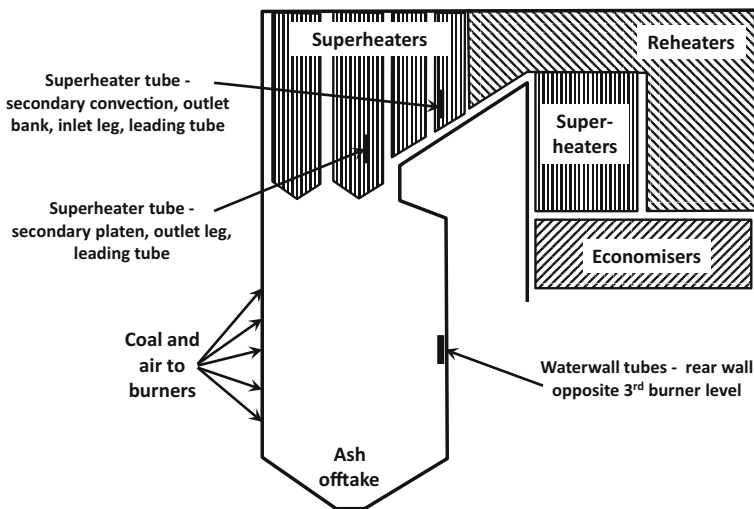


Fig. 1 Cross-section through power station unit showing the locations of trial-coated tubes

(OD) = 63.5 mm and wall thickness (W) = 7.1 mm joined together with 10 mm wide membranes, was installed into the rear furnace wall opposite the third burner row (Fig. 1). For the superheaters, individual tubes ~ 2 m long were installed into: (a) the leading tube of the secondary platen superheater (2.25 wt% Cr, OD = 51 mm, W = 8.8 mm), outlet leg; and, (b) the secondary convection superheater, outlet bank, inlet leg (316 stainless steel, OD = 44.5 mm, w = 6.4 mm).

Candidate Coatings

The candidate coatings were applied using either high-velocity oxy-fuel (HVOF) or arc-wire spraying. The HVOF coatings were applied by a commercial coating supplier using powders supplied by Sulzer Metco, with original powder compositions as shown in Table 1. Before their installation, a selection of the HVOF and arc-wire coatings had a candidate commercial sealant coating applied (based on a phosphate solution which was reacted with the coating surface) [8]. This sealant process was designed to close coating surface breaking pores, preventing the combustion environment from gain access to any internal voids in the coating. Additional samples of the HVOF coatings were sprayed in order to provide reference data for the as-sprayed condition of the coating.

Tubes 2/3/4 and 7/8/9 of the furnace wall panel were externally coated with approximately 200-mm long bands of alloy 625 (arc-wire sprayed), NiCrAlY, alloy 625, Cr_3C_2 in Ni–Cr matrix, FeCrAl, alloy 276 and Ni-50Cr (Fig. 2). With the exception of the alloy 625 applied by arc-wire spraying, all coatings were applied using HVOF. Tubes 2/3/4 also had the seal coating applied on top of the bands of coating. Tubes 1, 5, 6 and 10 were not coated. It should be noted that the tubes had already been assembled into a section of furnace wall panel, and so this restricted access for the coating processes and resulted in coatings that were thicker at the tube crowns (see Results).

The tubes for installation in the primary platen superheater, outlet leg, and the secondary convection superheater, outlet bank, inlet leg, were externally coated with bands approximately 100 mm long of arc-wire sprayed alloy 625, NiCrAlY, HVOF alloy 625, Cr_3C_2 in a Ni–Cr matrix, Ni-50Cr, alloy 276 and Ni-50Cr which were repeated once along the length of the tube (Fig. 3). These coatings were applied evenly around the individual tubes. One set of coatings had an additional seal coat (Fig. 3).

Plant Operating Data and Fuel Analyses

Operating data for this plant unit have been gathered throughout the exposure trials with the aim of enabling materials performance to be correlated with plant and component operating conditions. The coated samples were exposed for 24,880 operating hours.

The analyses of the fuels used in the plant are summarised in Table 2, and include the mean, maximum, minimum and standard deviation values for each

Table 1 Compositions of the powders used to produce the HVOF coatings

Coating label	Composition (Wt%)										Material code
	Al	C	Cr	Fe	Mn	Mo	Ni	Si	Others		
Ni-50Cr		0.1	46.0	1.1			Bal	2.1	$O < 0.03$		AE 9796
FeCrAl	5.9	0.03	21.7	Bal	0.76			0.83	$P < 0.01, S < 0.01$		AE 9797
NiCrAlY	9.9		22.0				Bal		$Y = 0.9, O < 0.02$		AE 9798
NiCrMoWFe (alloy 276)	0.05	0.01	15.6	4.01	0.38	15.4	Bal	0.31	$W = 4.51, Ti < 0.02,$ $N < 0.06, O < 0.03$		AE 9805
Cr ₃ C ₂ -NiCr matrix		7.7	56.1	0.2			35.2	0.1			AE 9806
NiCrMo(Nb + Ta) (alloy 625)	0.2		21.3	0.1		8.9	Bal	0.13	$Nb + Ta = 3.58, Cu = 0.18,$ $Co = 0.1, N < 0.03$		AE 9807

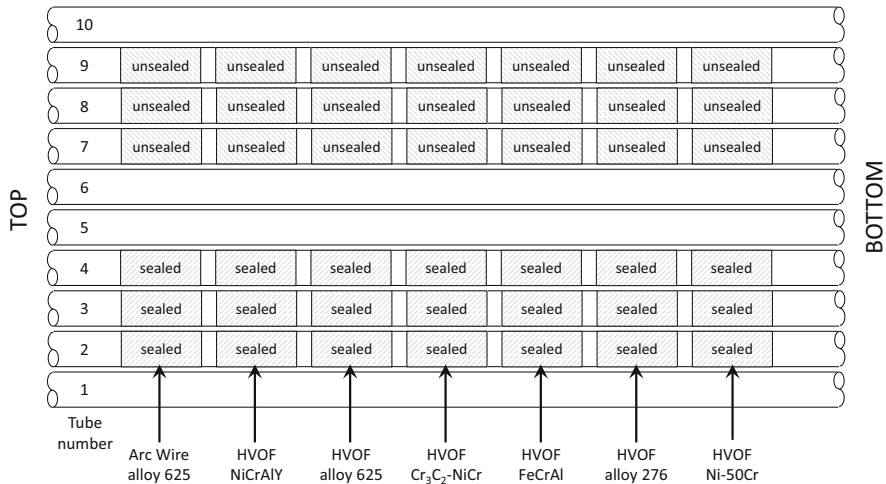


Fig. 2 Coating distribution on waterwall panel—all applied by HVOF except one by arc-wire spray

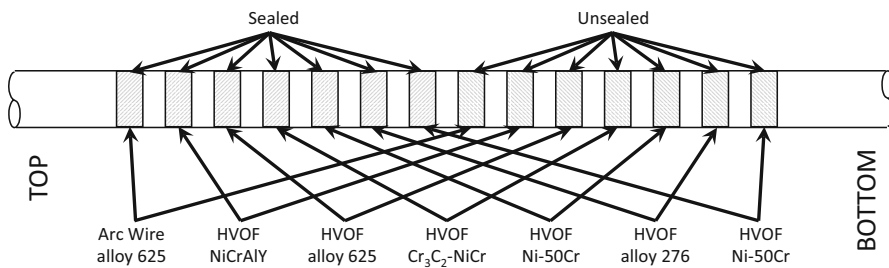


Fig. 3 Coating distribution on the primary platen superheater outlet leg and secondary convection superheater outlet bank inlet leg

Table 2 Fuel analyses for coals used during trial-coating exposures (as-received basis)

Parameter	Units	Max	Mean	Min	SD
Moisture	%	25.5	13.1	3.3	3.4
Volatiles	%	37.7	29.9	13.3	4.1
Fixed carbon	%	59.5	44.7	22.2	4.7
Ash	%	49.2	12.4	3.5	6.7
Calorific value	MJ kg ⁻¹	30.0	24.9	11.2	2.7
Sulphur	%	3.37	1.38	0.22	0.55
Chlorine	%	0.58	0.11	<0.01	0.11
Hydrogen	%	4.76	3.93	1.56	0.48

parameter. These gave combusted gas compositions with mean values of 4 vol% O₂, 2900 mg/m³ SO₂, 390 mg/m³ NO_x and 160 mg/m³ CO.

The average steam drum pressure during the exposures was 172 bar with variations from ~132 to 197 bar; this corresponds to a mean saturation temperature

of 354 °C, with a range of 333–365 °C. Furnace wall metal temperatures are not only greatly influenced by the internal saturated steam temperature but also by the incident heat flux, this again being greatly influenced by the burners which are in operation and the extent of furnace wall ash fouling. With a nominal wall thickness of 7 mm and a heat flux variation of 200–500 kW/m², there are significant uncertainties in estimating the mean waterwall tubes surface metal temperatures. However, if a nominal 400 kW/m² is assumed, then this equates to a thermal gradient of ~9 °C/mm, and gives an estimated surface metal temperature of ~420 °C. For the superheaters, from the plant unit monitoring system, estimates of the mean surface temperatures during periods of normal operation were: (a) 485 °C for the leading tube of the secondary platen superheater outlet leg; and (b) 560 °C for the secondary convection superheater, outlet bank, inlet leg.

Coating Monitoring and Performance Assessment

Prior to their installation, the thicknesses of the coatings on the tubes were measured using an Elcometer film thickness gauge for the non-magnetic coatings on the ferritic tubes and callipers on the austenitic tubes. For each coating on the furnace wall panel, measurements were taken at five locations around the tubes (so that position 3 corresponded to the tube ‘crown’ or 12 o’clock position) and at three points along the tube (edges and centre).

For coatings on the ferritic superheater tube, measurements were taken at the 12, 3, 6 and 9 o’clock positions (with 12 o’clock corresponding to the centre of the upstream surface) at three location along the coating length (edges and midpoint). On the austenitic superheater tube, two measurements were taken for the diameter at 90° relative to each other and repeated at three locations along the coating length. The uncoated tube diameter was deducted from the measurements to determine the coating thickness.

Cross-sections were prepared through all reference samples and exposed tube samples, using non-aqueous preparation methods to preserve any adherent water-soluble surface deposits. For reference samples, a visual assessment of the coating oxide and voidage content was made as previous work with plasma sprayed corrosion resistant coatings had shown that improved corrosion resistance was linked to reduced oxide and voidage contents.

Results and Discussion

As-Sprayed Coating Characterisation

Examples of the coating microstructures generated are shown in Fig. 4. The fine structure associated with the HVOF coatings rendered accurate assessment of the oxide and voidage content difficult with the normal optical digital image analysis routines used to assess plasma-sprayed coatings, so SEM/EDX techniques had to be used instead. In general, the coatings exhibited low oxide and porosity contents. These were significantly below the 12% combined oxide and voidage content and

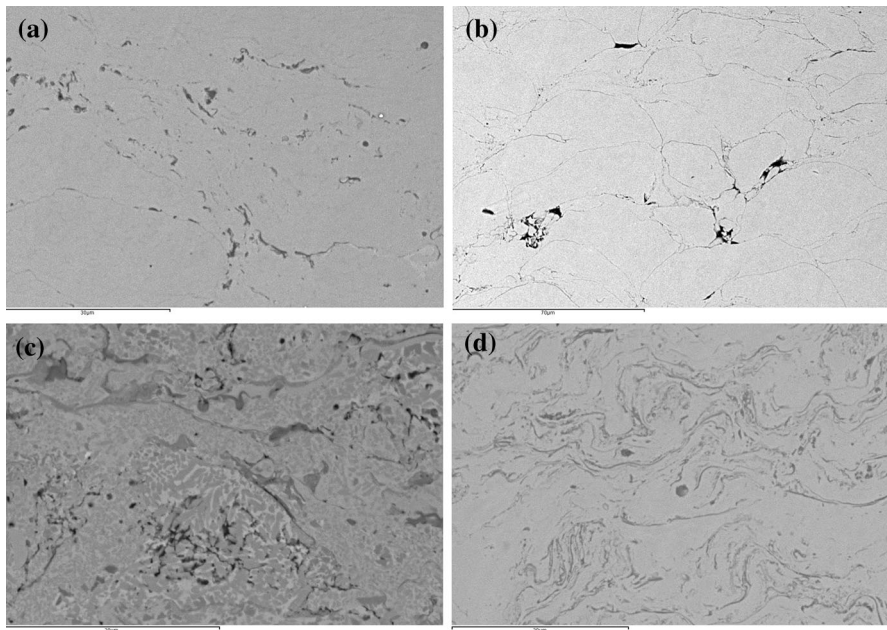


Fig. 4 Representative microstructures of different as-sprayed HVOF coatings. The images have been selected to illustrate the variations in coating microstructures observed. **a** Ni-50Cr, **b** FeCrAl, **c** Cr₃C₂-NiCr matrix, **d** alloy 625 NiCrMo(Nb+Ta)

1% voidage previously considered necessary to ensure good coating performance. One exception to this was for the alloy 625 coating which was observed to contain a unusually high oxide content (Fig. 4d). The Cr₃C₂-filled NiCr matrix coating contained a considerable amount of the hard, erosion-resistant carbide material as expected (Fig. 4c), although this prevented the assessment of its oxide and porosity content.

Coatings Exposed on Waterwall Tubes

The cross-sections through the exposed samples showed that all of the coatings had experienced fireside corrosion on their surfaces at the crown (i.e. 12 o'clock positions), but only the HVOF alloy 625 coatings had disappeared completely (both unsealed and sealed variants, as shown in Figs. 5, 6). However, looking around the tube surfaces, it was clear that many of them had failed towards the 'sides' of the tubes (i.e. at angles greater than $\sim 60^\circ$ to tube 'crown'); this is shown in Fig. 7 for a sealed FeCrAl sample, with no coating left on the right 'side' of the tube. SEM/EDX analyses of samples were carried out to confirm the coating identities. These examinations also characterised the deposit compositions that had formed on the tube surfaces and that the corrosion damage morphologies were consistent with typical waterwall corrosion damage for a coal-fired boiler [7].

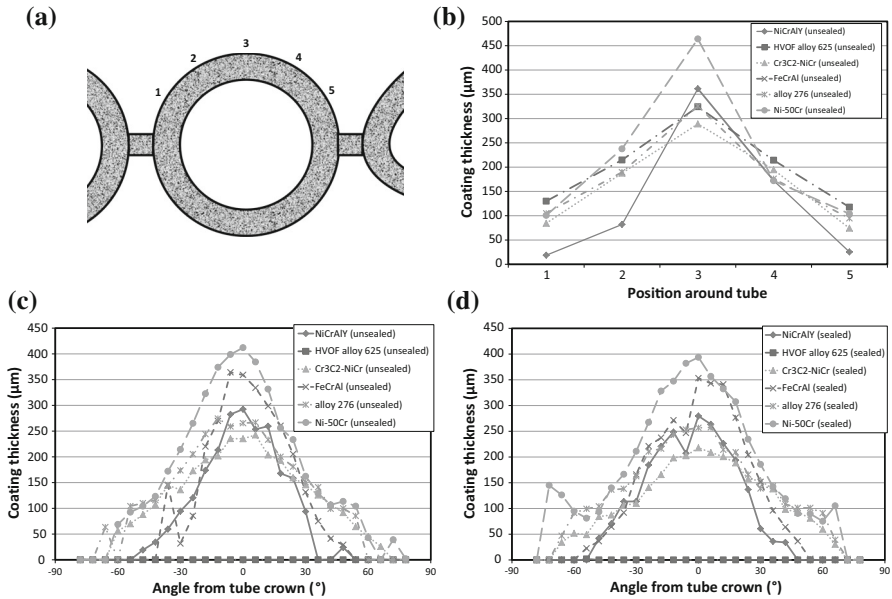


Fig. 5 Variation in unsealed HVOF coating thickness around waterwall tubes 3 and 8 before and after exposure. **a** pre-exposure measurement positions, **b** before exposure, **c** after exposure—unsealed coatings, **d** after exposure—sealed coatings

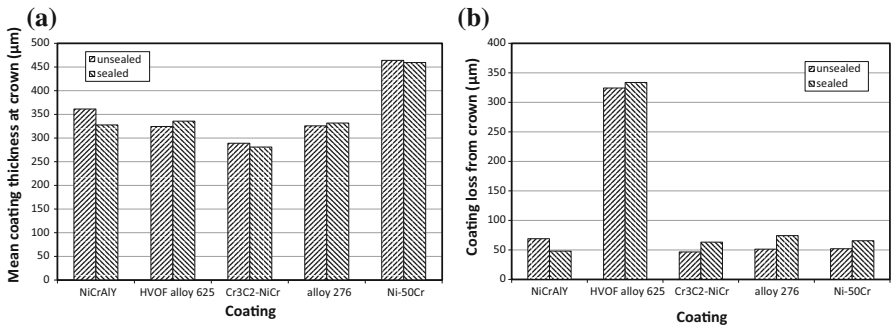


Fig. 6 Pre- and post-exposure HVOF coating thicknesses on waterwall tubes 3 and 8 (except FeCrAl as no pre-exposure data). **a** Mean coating thicknesses at waterwall tube ‘crowns’, **b** coating losses from waterwall tube ‘crowns’

Dimensional metrology measurements were carried out on all the coated tubes before and after their exposures. Figure 5b shows the data generated by pre-exposure Elcometer measurements at the five radial locations for each of the unsealed coatings on tube 8. This illustrates the initial variation in the thickness of these coatings around the tubes. After exposures, measurements of coating thicknesses were carried out at 6° intervals around the tube cross-sections. The results of these are shown in Fig. 5c for the same tube 8 coatings and in Fig. 5d for an unsealed version of the same coatings (tube 3).

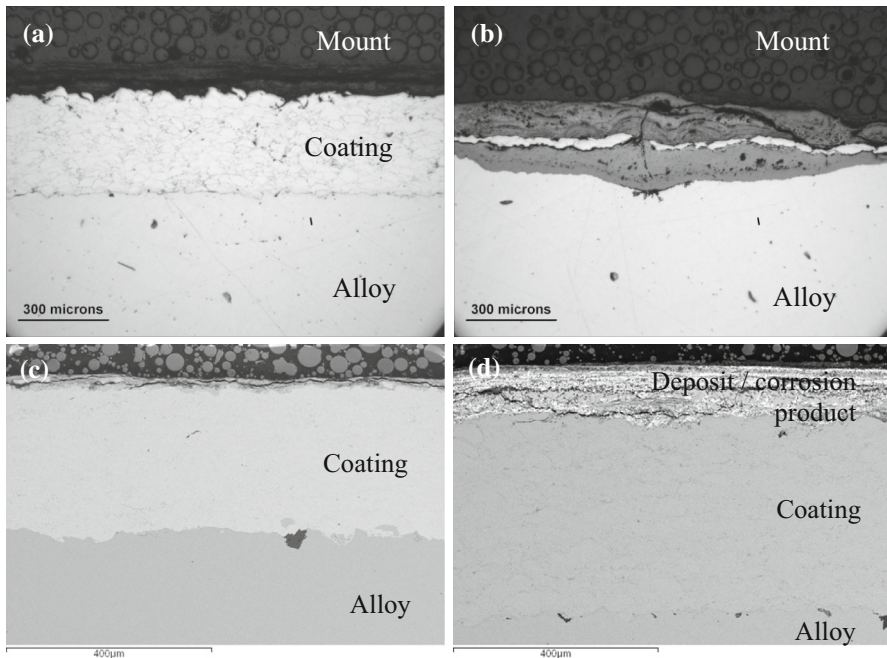


Fig. 7 Examples of variation in appearance of coated waterwall tubes after exposure (more detailed coating thickness information shown in Fig. 5). **a** ‘Crown’ of HVOF FeCrAl waterwall tube, **b** right side of HVOF FeCrAl waterwall tube, **c** ‘crown’ of HVOF alloy 276 waterwall tube, **d** ‘crown’ of Ni-50Cr waterwall tube

These data emphasise the much greater coating thicknesses in the ‘crown’ areas (or 12 o’clock positions) which are shown at zero degrees on the x -axis in Fig. 5c, d, and the tailing off of the coating thicknesses on either side of this peak position. These data should be compared to those generated by the pre-exposure metrology (e.g. Fig. 5b), which showed the coatings becoming thinner away from the ‘crown’ areas (i.e. either side of position 3 in Fig. 5a). It is clear that the areas of thinner coatings have failed during the course of exposures in the plant. Given the variation in coating thicknesses around the tubes that has resulted in areas of total coating loss, to obtain quantitative data on coating performances it is necessary to use the maximum coating thickness measurements (corresponding to the tube ‘crowns’) before and after exposure.

Figure 6 shows the coating losses calculated for each of the coatings with and without sealant layers. As there is no HVOF IN625 coating left in either case, it has clearly performed the worse, with corrosion damage exceeding the 320–330 μm coating thicknesses. However, all the other coatings have performed similarly with damage levels of ~ 50 to $75 \mu\text{m}$ during their ~ 25 khour exposure (i.e. ~ 2 – $3 \mu\text{m}$ per 1000 h). There was no obvious benefit from the sealant—for the majority of the coatings the sealed version had apparently corroded a little more than the unsealed version (but this was within the standard deviation of the measurements).

Coatings Exposed on Superheater

Similar examinations were carried out for the coatings exposed on the superheater tubing. SEM/EDX examinations of the cross-sections through the coatings confirmed the coating compositions. These examinations also characterised the deposit compositions that had formed on the tube surfaces and that the corrosion damage morphologies (e.g. Fig. 8) were consistent with typical superheater corrosion damage for a coal-fired boiler [7].

Figure 9a shows the thicknesses of the sealed coatings after their exposure. This shows that only HVOF Ni-50Cr had survived on the upstream surface of the tubes,

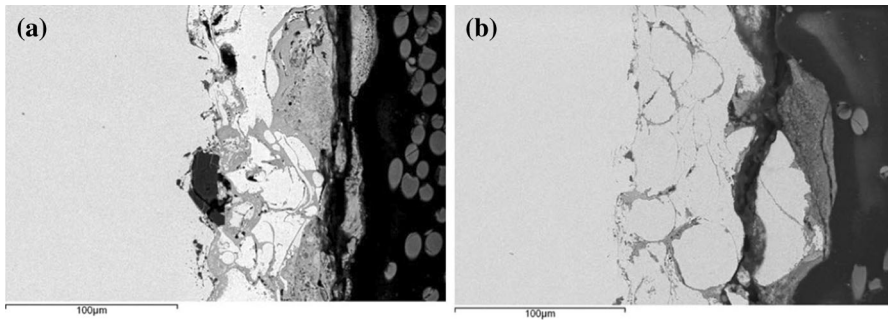


Fig. 8 Summary of coating performances on the superheater, **a** arc wire alloy 625 3 o'clock position, **b** HVOF NiCrAlY 3 o'clock position

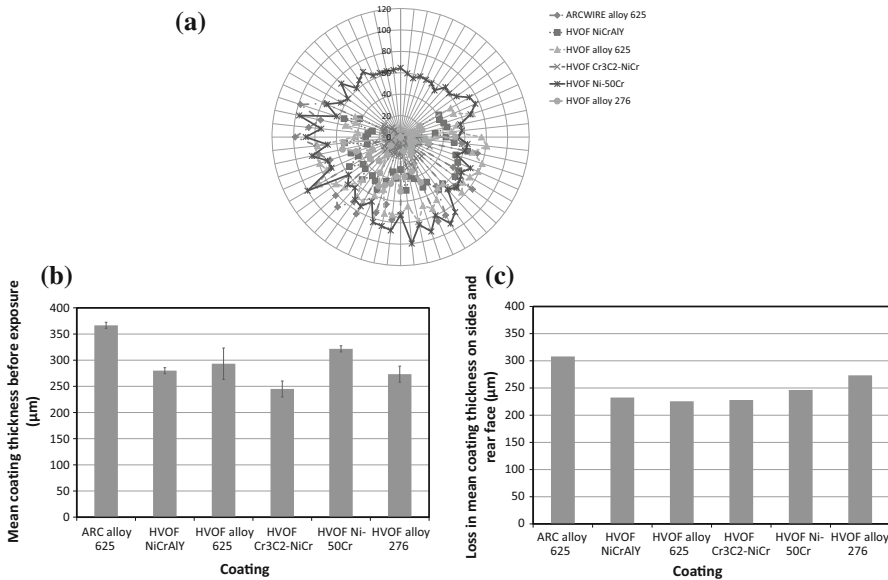


Fig. 9 Examples of coating performances on the superheater. **a** Coating thicknesses (µm) as a function of radial position around superheater (upstream tube face at top), **b** mean coating thicknesses before exposure on the superheater, **c** mean loss in coating thicknesses from the sides and downstream faces during exposure on the superheater

but all the coatings were present around the rest of the tube surfaces. Pre-exposure coating measurements were in the range ~ 250 to $350\ \mu\text{m}$ (Fig. 9b), with some coatings having initial thicknesses on average $100\ \mu\text{m}$ less than others (the bars in this figure show the standard deviations of the initial coating measurements). Figure 9c shows the differences between the average coating thicknesses before exposure for these samples and those measured on the sides/downstream surfaces of the samples after exposure. Given the spread in the measurement datasets, the results for the HVOF coatings, with thickness losses of ~ 220 to $260\ \mu\text{m}$, indicate similar levels of behaviour (i.e. ~ 9 to $10\ \mu\text{m}$ per 1000 h). However, the arc-wire alloy 625 coating performed worse with an average downstream coating thickness loss of $\sim 300\ \mu\text{m}$ (i.e. $\sim 12\ \mu\text{m}$ per 1000 h).

Conclusions

Following the exposure of candidate protective coatings for heat exchanger tubes in a 500 MWe unit of a UK pulverised coal-fired power station for ~ 25 khours, the following main conclusions can be drawn:

For both the waterwall and superheater locations, the performance of the range of commercial coatings (six HVOF systems and one arc-wire system) depended on the quality of the applied coating rather than its composition. The use of a phosphate-based sealant system did not improve the performance of the coatings in either location in this unit.

On the waterwalls, it was found that the HVOF IN625 coatings were not present after their exposure. For the other coatings, similar damage levels of ~ 50 – $75\ \mu\text{m}$ were observed at the tube ‘crown’ (i.e. ~ 2 to $3\ \mu\text{m}$ per 1000 h). However, the wide range in initial coating thicknesses meant that some of the coatings had failed towards the sides of the tubes where they were all initially significantly thinner (due to the coating application methods used).

On the superheaters, it was found that the only coating that had survived on the upstream tube faces was Ni-50Cr. However, for the rest of the tube surfaces, on average all the coatings all had similar levels of damage at ~ 220 to $260\ \mu\text{m}$ (i.e. ~ 9 to $10\ \mu\text{m}$ per 1000 h), except for arc-wire IN625 which was higher at $\sim 300\ \mu\text{m}$ (i.e. $\sim 12\ \mu\text{m}$ per 1000 h).

Given the low loss rates for well-applied coatings in these two component environments, whether or not to use such coatings depends on the ability to apply coatings that are thick enough to last between maintenance intervals, coating cost and quality control, as well as the costs associated with alternative solutions. These will vary between boiler operator, coating supplier and country. In addition, the coal composition/quality and particular boiler operating conditions also need to be taken into account.

Acknowledgements The authors gratefully acknowledge funding for the research reported in this paper from the UK Technology Strategy Board Project “Advanced Surface Protection Enabling Carbon Abatement Technologies” (ASPECT, Project number TP11/MFE/6/1/AA140E) and the EU FP7 Project “Meeting the Materials and Manufacturing Challenge for Ultra High Efficiency PF Power Plants with CCS” (NEXTGENPOWER, Project ENER/FP7EN/249745).

Open Access This article is distributed under the terms of the Creative Commons Attribution 4.0 International License (<http://creativecommons.org/licenses/by/4.0/>), which permits unrestricted use, distribution, and reproduction in any medium, provided you give appropriate credit to the original author(s) and the source, provide a link to the Creative Commons license, and indicate if changes were made.

References

1. EC. *LIFE and Climate Change Mitigation* (European Union, Brussels, 2015).
2. A. F. Stam, NextGenPower—demonstration and component fabrication of nickel alloys and protective coatings for steam temperatures of 750°C, in *Proceedings of the 7th International Conference on Advances in Material Technology for Fossil Power Plants* (EPRI, Hilton Waikoloa Village, Hawaii, 2013).
3. N. J. Simms, et al., *Materials Science and Technology* **29**, 804 (2013).
4. R. Viswanathan, R. Purgert, and P. Rawls, *Advanced Materials and Processes* **166**, 47–49 (2008).
5. J. P. Shingledecker and I. G. Wright, in *Materials for Power Engineering 2006*, eds. J. Lecomte-Beckers et al (Forschungszentrum Jülich, Jülich, 2006), p. 107
6. T. Lant et al., Modeling fireside corrosion of heat exchanger materials in advanced energy systems, in *Proceedings of the 6th International Conference on Advances in Material Technology for Fossil Power Plants (EPRI)*, (ASM International, Santa Fe, New Mexico, 2011), pp. 255–267
7. N. J. Simms, Environmental degradation of boiler components, in *Power Plant Life Management and Performance Improvement*, ed. J. E. Oakey (Woodhead Publishing, Sawston, 2011), pp. 145–179.
8. M. Oksa, E. Turunen, and T. Varis, Sealing of thermally sprayed HVOF coatings for boiler applications, in *Thermal Spray 2004: Advances in Technology and Applications* (ASM International, Santa Fe, New Mexico, 2004), pp. 120–124.